JEE Journal of Ecological Engineering

Journal of Ecological Engineering, 2025, 26(12), 65–81
https://doi.org/10.12911/22998993/208436
ISSN 2299–8993, License CC-BY 4.0

Received: 2025.07.10
Accepted: 2025.09.01
Published: 2025.10.01

Production of activated carbon from macadamia nut shell waste for phenol removal using a partial-bed adsorption system

Thanakrit Pongsak[1], Mananya Phalaiphai[1], Watcharapol Wonglertarak[2], Maturada Khowattana[1], Boonchai Wichitsathian[1], Jareeya Yimrattanabovorn[1*]

[1] School of Environmental Engineering, Institute of Engineering, Suranaree University of Technology, Nakhon Ratchasima, Thailand
[2] Environmental Engineering and Disaster Management Program, School of Interdisciplinary Studies, Mahidol University, Kanchanaburi Campus, Kanchanaburi, Thailand
* Corresponding author's e-mail: chareeya@sut.ac.th

ABSTRACT

Phenolic compounds, commonly found in industrial wastewater from oil refining and petrochemical processes, pose significant environmental and health risks due to their toxicity and resistance to biological degradation. Among the various treatment methods, adsorption is particularly effective owing to its high efficiency and low generation of harmful by-products. However, the widespread use of commercial activated carbon is limited by its high cost. In this study, macadamia nut shells – an abundant agricultural waste – were utilised to produce low-cost macadamia nut shell activated carbon (AC-M) via CO_2 activation. The optimal activation conditions (200 mL/min CO_2 flow, 950 °C, 240 minutes) yielded AC-M with a high BET surface area of 1,363.75 m^2/g and predominantly featuring micro- to mesopores in range of 2.06–2.36 nm. Batch adsorption experiments revealed optimal conditions for phenol removal at an initial concentration of 200 mg/L, contact time of 600 minutes, pH 6 (favourable hydrophobic interaction), and 25 °C, indicating an exothermic process. Equilibrium data closely followed the Langmuir isotherm ($R^2 > 0.97$), with a maximum adsorption capacity of 588.24 mg/g for the best-performing AC-M ($AC\text{-}M_{200\,240}$). A key innovation in this study is the application of a partial-bed column system, which periodically replaces saturated adsorbent to maintain an active mass transfer zone. Compared to a traditional fixed-bed column, the partial-bed significantly extended operational time and improved performance. At a 6 cm removal height, the partial-bed achieved 124 hours of operation lifespan in the third cycle over three times longer than the 39 hours observed in a 10 cm fixed-bed column, while enhancing adsorption capacity to 246.70 mg/g, a 44% increase in efficiency. These findings demonstrate that the integration of low-cost AC-M with a partial-bed column system offers a promising, sustainable, and highly efficient solution for continuous phenol removal from industrial wastewater.

Keywords: phenol adsorption, macadamia nut shell waste, activated carbon, partial-bed column, lifespan of column.

INTRODUCTION

Phenol and its derivatives are widespread pollutants released into the environment by diverse industries, including petrochemical, rubber, plastics, pharmaceutical, and pesticide manufacturing (Said et al., 2021). Even at trace concentrations, these compounds pose significant public health risks due to their high toxicity, potential carcinogenicity, and ability to impart undesirable taste and odour to drinking water and other water supplies. Chemically, phenol (C_6H_5OH) is an aromatic compound characterised by a hydroxyl group directly bonded to an aromatic carbon ring, rendering it particularly recalcitrant to removal by conventional wastewater treatment methods.

Numerous technologies have been developed to remediate phenol-contaminated wastewater, such as biological treatment, ozonation (Saputera et al., 2021), electrochemical oxidation (Said et al., 2021; Xu et al., 2024), and adsorption (Eryılmaz and Genc, 2021; Mohd, 2022). However, some of these methods present challenges, including the risk of bioaccumulation or the formation of harmful

by-products. Among the available options, adsorption utilising activated carbon is widely favoured for its high efficiency, operational flexibility, and the absence of toxic by-products. Despite these advantages, the substantial cost of commercial activated carbon often restricts its broader application.

To address the economic constraints associated with commercial adsorbents, significant attention has been directed towards developing low-cost activated carbon from agricultural waste materials, which are known for their high surface area and effectiveness in pollutant removal (Patel, 2020). Previous research has, for instance, successfully demonstrated that the activated carbon derived from macadamia nut shells possesses considerable adsorption capacities for various contaminants in wastewater (Wongcharee et al., 2018; Yimrattanabovorn et al., 2024). This offers a promising avenue for valorising agricultural by-products into valuable adsorbents.

For industrial-scale applications, the continuous fixed-bed adsorption technique is commonly preferred due to its inherent simplicity and ease of scaling up (Mesfer et al., 2020). Nevertheless, fixed-bed columns are susceptible to limitations such as clogging and a decline in efficiency over time, necessitating frequent replacement of the adsorbent material. This often leads to lower adsorption capacities when compared to batch systems and can result in the underutilisation and wastage of the adsorbent bed (Patel, 2019; Sazali et al., 2020).

This research proposed an advanced technique, the partial-bed column adsorption system, engineered to substantially boost adsorption performance. Within this dynamic setup, less efficient, partially spent sections of the adsorbent bed are precisely extracted and replenished with either fresh or reactivated adsorbent. This adaptive methodology facilitates a more thorough utilisation of the adsorbent, leading to reduced overall material usage and, consequently, a prolonged operational lifespan for adsorbents in continuous column operations (Patel, 2019; Plangklang and Sookkumnerd, 2023; Yimrattanabovorn et al., 2024).

The objective of this study was to assess the feasibility of employing activated carbon derived from macadamia nut shells for the removal of phenol, using both batch and column adsorption experiments. This work underscores the potential of agricultural waste as an economical adsorbent. The batch experiments explored the impact of significant parameters, including phenol concentration, contact time, pH, temperature, and adsorption isotherms. The packed-bed column experiments examined breakthrough curves and related performance metrics under varying phenol concentrations, flow rates, and layer heights. The findings from the packed-bed column experiments contribute valuable guidance for optimising operating conditions in industrial applications, particularly for implementing partial-bed column systems. Overall, this study offers viable approaches for large-scale water purification, highlighting the efficiency and long-term applicability of macadamia nut shell–derived activated carbon in removing phenol.

MATERIALS AND METHODS

Materials

Macadamia nut shell charcoal, serving as the raw material for this study, was sourced from Chiang Rai province, Thailand. This charcoal underwent size reduction through crushing, followed by sieving to achieve a particle size range of 1.70 to 2.38 mm, in accordance with ASTM (2004) standards.

The intrinsic proximate and thermal decomposition properties of the prepared macadamia nut shell charcoal were comprehensively assessed using a Mettler Toledo TGA/DSC1 instrument for thermogravimetric analysis (TGA). For the proximate analysis, the samples were initially heated to 110 °C at 10 °C/min under an inert nitrogen (N_2) atmosphere for 30 minutes to quantify their moisture content. Subsequently, the temperature was raised to 850 °C under N_2 for 7 minutes to determine the volatile matter. Finally, the temperature was lowered to 800 °C, and an oxygen (O_2) gas flow (10 °C/min for 20 minutes) was introduced to ascertain the percentages of fixed carbon and ash.

Preparation of macadamia activated carbon

Macadamia activated carbon (AC-M), utilised as the adsorbent in this study, was synthesised from the prepared macadamia nut shell charcoal using a horizontal tubular furnace (CTF 12/75/700/201, Carbolite Gero Ltd., Hope Valley, UK). The activation parameters were optimised based on the insights from TGA analysis and authors' prior research. Specifically, the activation process was conducted at a constant temperature of 950 °C. CO_2 gas was introduced at flow rates of 100 and 200 mL/min for varying durations of

60, 120, 180, and 240 minutes. Prior to activation, the sieved macadamia nut shell charcoal samples were loaded into a ceramic boat and positioned within the furnace. The furnace temperature was gradually ramped up to 950 °C at a heating rate of 5 °C/min under a continuous nitrogen (N_2) flow of 100 mL/min. Upon reaching the target temperature, the N_2 flow was replaced with CO_2 gas at the designated flow rate and activation time. After the activation period, the AC-M samples were allowed to cool to room temperature under a protective nitrogen atmosphere. For clarity in reporting, each prepared AC-M sample was systematically labelled in the format "AC-$M_{\text{flow rate.time}}$", where flow rate denotes the CO_2 flow rate (mL/min) and time represents the activation duration (minutes). For example, "AC-$M_{200.240}$" signifies a sample activated with CO_2 at 200 mL/min for 240 minutes. The surface characteristics of the prepared AC-M samples were analysed using the Brunauer-Emmett-Teller (BET) technique. Measurements of specific surface area were conducted with a BET Sorp mini II analyser (Japan).

Preparation of phenol solution

Phenol crystals utilized in this study were of high purity (99.5%) and were of AR/ACS grade, procured from Loba Chemie. A standard phenol solution was prepared in the form of C_6H_5OH with a concentration of 1,000 mg/L, using distilled water for dilution. The maximum absorbance wavelengths at 270 nm were determined using a UV-Visible spectrophotometer (JENWAY 7315, UK) for all experiments to ascertain the concentration of phenol.

Batch adsorption studies and adsorption isotherm models

For the adsorption studies under batch conditions, 250 ml Erlenmeyer flasks were used, each filled with 200 ml of phenol solution. The flasks were incubated in a temperature-controlled shaker to ensure stable experimental conditions. The experiments were designed to examine the effects of initial phenol concentration (50–300 mg/L), contact time (60–780 minutes), initial pH (2–12), and temperature (25–45 °C) on the adsorption performance of AC-M. The initial (C_0) and equilibrium (C_e) concentrations of phenol were analysed to evaluate the adsorption performance of the AC-M. The equilibrium adsorption capacity, q_e (mg/g), was determined using Equation 1, where V is the volume of the phenol solution (in mL) and m is the mass of the AC-M used.

$$q_e = \frac{(C_0 - C_t)V}{W \times 1000} \quad (1)$$

To elucidate the equilibrium behaviour of phenol adsorption onto the AC-M samples, the experimental data from batch studies were fitted to two widely recognised adsorption isotherm models: Langmuir and Freundlich. These models mathematically describe the relationship between the amount of adsorbate adsorbed onto the adsorbent at equilibrium (q_e) and the equilibrium concentration of the adsorbate in the solution (C_e). The linearized form of the Langmuir isotherm is given by Equation 2.

$$\frac{C_e}{q_e} = \frac{C_e}{q_m} + \frac{1}{K_L q_m} \quad (2)$$

where: q_m represents the maximum adsorption capacity (mg/g), corresponding to the amount of adsorbate required to form a complete monolayer on the adsorbent surface. K_L is the Langmuir constant (L/mg), which is indicative of the affinity of the binding sites.

Conversely, the Freundlich isotherm model describes multilayer adsorption on heterogeneous surfaces, assuming that adsorption sites possess varying adsorption energies, with stronger binding sites being occupied preferentially. The linearized form of the Freundlich isotherm is expressed by Equation 3.

$$\log q_e = \log K_F + \frac{1}{n} \log C_e \quad (3)$$

In this equation, K_F is the Freundlich constant $(mg/g)(L/mg)^{1/n}$, reflecting the adsorption capacity, and n is the Freundlich exponent, which signifies the adsorption intensity or the heterogeneity of the adsorbent surface.

Column adsorption studies

Investigation of adsorption in a fixed-bed column system

The fixed-bed column adsorption experiments were performed using a cylindrical acrylic vessel with an diameter of 2 cm with a vertical length of 10 cm, as depicted in Figure 1.

A continuous up-flow operation was maintained throughout the experiments using a peristaltic pump to ensure a constant flow rate. The pH of the influent phenol solution was consistently adjusted to 6 ± 0.2 using either 0.1 M NaOH or 0.1 M HCl. All fixed-bed experiments were conducted at ambient temperature.

The experiments were carried out under varying operational conditions, including different initial phenol concentrations (150, 200, and 250 mg/L) and flow rates (4, 5, and 6 mL/min). The main aim of this study was to examine continuous-flow adsorption process by analysing critical values on the breakthrough curve specifically, where 95% of phenol is removed (C_e/C_o = 0.05) and where only 5% removal occurs (Ce/Co = 0.95). Throughout the process, the phenol concentration in the effluent (Ct) was continuously measured to evaluate the system's performance. Breakthrough curves were generated by plotting C_t/C_0 versus time (t), and essential parameters were calculated, including breakthrough time (t_b), saturation time (t_s), effluent volume (V_{eff}), adsorption capacity at breakthrough (q_b), and adsorption capacity at saturation (q_s) were calculated.

Partial-bed column study

The partial-bed column adsorption experiments were conducted following the procedures outlined in Figure 1, utilising optimal conditions previously established from the fixed-bed column study. This investigation systematically examined how varying removed partial-bed heights (4, 5, and 6 cm) influenced the adsorption capacity of the column and its operational lifespan. In this partial-bed column, a critical operational criterion was implemented: the adsorbent bed was replenished specifically when the removal efficiency dropped to 50% (C_e/C_0 = 0.50). Upon reaching this point, the corresponding spent portion of AC-M was removed, and an equivalent amount of fresh AC-M was introduced from the top of the column. Each experiment comprised a total of three cycles, and key breakthrough curve parameters were subsequently calculated for each cycle to comprehensively evaluate the overall performance of the system.

Analysis of breakthrough curves models

To thoroughly assess the dynamic behaviour of phenol adsorption in both fixed-bed and partial-bed column configurations, the experimental breakthrough data were interpreted using two widely recognised models: the Thomas and Yoon–Nelson models. These modelling approaches offer critical understanding of the adsorption kinetics and breakthrough behaviour, serving as essential tools for forecasting column performance and supporting the development of large-scale adsorption systems.

The Thomas model is widely applied to describe fixed-bed adsorption processes, operating under the assumptions that external and internal

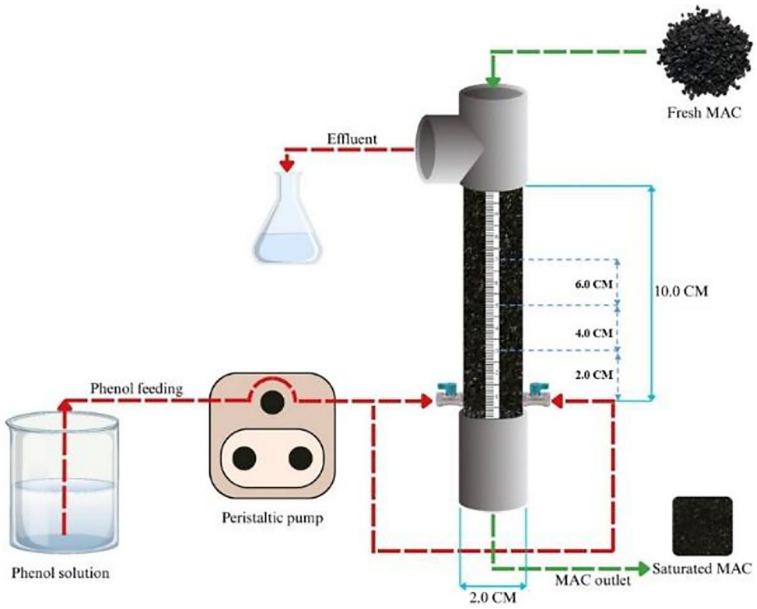

Figure 1. A schematic diagram of column study

mass transfer resistances are negligible and that the adsorption kinetics follow the Langmuir isotherm. Its linearized form is expressed by Equation 4.

$$ln\left(\frac{C_0}{C_t}-1\right)=\frac{K_{TH}q_{TH}m}{Q}-K_{TH}C_0t \qquad (4)$$

where: C_t represents the concentration of phenol (mg/L) at any given time t (min), C_0 is the initial phenol concentration (mg/L), m is the weight of the AC-M adsorbent used in the column (g), and Q is the feed flow rate (mL/min). K_{TH} and q_{TH} represent the Thomas rate constant (mL/mg·min) and the equilibrium phenol uptake (mg/g), respectively.

The Yoon-Nelson model, in contrast, offers a simpler approach that does not necessitate detailed information regarding adsorbate properties or bed characteristics. It posits that the rate of decrease in the probability of adsorption for each adsorbate molecule is directly proportional to both the probability of adsorbate adsorption and the probability of adsorbate breakthrough. The linearized form of the Yoon-Nelson model is given by Equation 5.

$$ln\left(\frac{C_t}{C_0\text{-}C_t}\right)=K_{YN}t\text{-}\tau K_{YN} \qquad (5)$$

where: K_{YN} represents the Yoon-Nelson rate constant (min^{-1}), t is time required for contaminant breakthrough (minutes), and τ is the time required for 50% adsorbate breakthrough (minutes).

RESULTS AND DISCUSSION

Characteristics of macadamia nut shell charcoal

The proximate analysis of the macadamia nut shell charcoal, which serves as the foundational material for the employed activated carbon, revealed key compositional data: a moisture content of 2.02%, volatile matter at 27.68%, fixed carbon at 65.24%, and an ash content of 5.06%. The significantly high fixed carbon content, combined with a relatively low ash content, strongly indicates that this agricultural waste is a highly promising precursor for producing activated carbon. This is critical because the fixed carbon content is essential for maintaining structural integrity and providing the necessary carbon mass throughout the activation process (Heidarinejad et al., 2020). To gain deeper insight into its thermal decomposition behaviour and to provide data to the adopted activation strategy for AC-M production, thermogravimetric analysis (TGA) was performed on the prepared macadamia nut shell charcoal. Figures 2A and 2B visually present the stepwise mass loss as a function of temperature and time, respectively.

As illustrated in Figure 2A, the mass loss profile across increasing temperatures clearly shows distinct decomposition stages, corresponding to the primary constituents of the biomass. Initially, a mass loss of 7.34% was recorded between 0–150 °C; this phase is primarily attributed to the evaporation of moisture. The most substantial mass reduction, amounting to 31.67%, occurred within the 150–900 °C range. This significant loss is consistent with the thermal breakdown of hemicellulose, cellulose, and lignin, which are known to decompose predominantly within this temperature window (Dittmann et al., 2022). Further details from Figure 2B show the cumulative mass loss over time. Approximately 87 minutes into the process, the charcoal had undergone a total mass loss of about 39.01%, after which the rate of mass loss declined sharply. On the basis of these TGA findings, the observed mass loss at 900 °C after 87 minutes suggests the conditions conducive to the development of a highly porous structure in the activated carbon, as a greater mass loss generally correlates with more extensive pore formation (Rasapoor et al., 2020). To further optimise this porous structure and maximise its potential for adsorption applications, we determined that more intensive activation conditions would be beneficial. Consequently, subsequent activation experiments were conducted at elevated temperatures of 900, 950, and 1000 °C, coupled with varied activation times ranging from 60 to 240 minutes, aiming to achieve the desired performance characteristics for our AC-M.

Preliminary evaluation of AC-M parameters

The physical characteristics of the AC-M, synthesised under various activation temperatures and durations, were meticulously assessed through BET analysis. The results of this analysis are comprehensively presented in Table 1, clearly indicate that an activation temperature of 950 °C

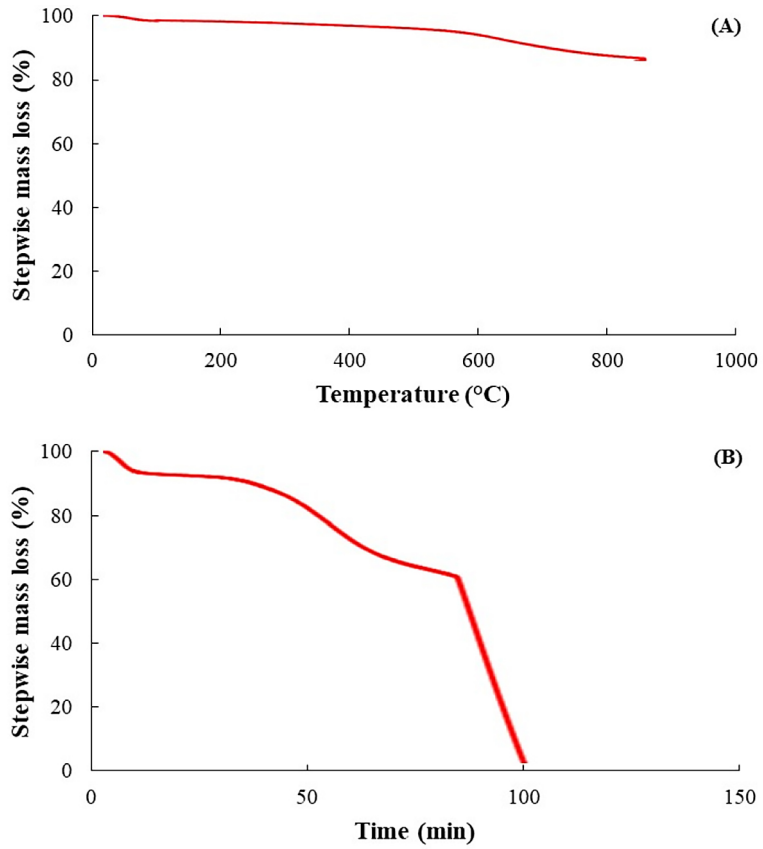

Figure 2. The effect of A) temperature and B) activation time for thermogravimetric analysis of AC-M

consistently yielded the highest surface area for the activated carbon when compared to the activations performed at 900 °C and 1000 °C. Furthermore, a discernible trend was noted: as the activation time increased, both the specific surface area (S_{BET}) and the total pore volume (V_{total}) of the AC-M samples generally increased. Conversely, prolonging the activation duration led to a decrease in the percentage yield of AC-M and a reduction in the mean pore diameter.

On the basis of these compelling preliminary findings, 950 °C was definitively selected as the optimal activation temperature for all subsequent experiments. This decision allowed for a focused investigation into other critical parameters for achieving desired activated carbon performance, specifically by varying the CO_2 flow rates (100 and 200 mL/min) and activation times (60–240 minutes).

Characterization of macadamia activated carbon

The porous properties of the synthesized AC-M samples underwent comprehensive evaluation using BET analysis, with the summarised results presented in Table 2. The crucial characteristics that directly influence the performance of an adsorbent include specific surface area, cumulative pore volume, and average pore size. As both the activation temperature and duration increased, a progressive loss of carbon content from the charcoal structure was observed, leading to a corresponding decrease in the overall yield. Specifically, the percent yield varied from 34.53% to 67.32% when a CO_2 flow rate of 100 mL/min was used, and from 31.33% to 66.68% with a CO_2 flow rate of 200 mL/min. This reduction in yield, observed with increased CO_2 flow rate and activation time, is attributed to intensified gasification reactions occurring between CO_2 and the carbon framework of the AC-M, resulting in greater carbon loss. The deliberate loss of carbon within the granular AC-M structure during the activation process is fundamental for the development of a large surface area and substantial total pore volume (Zhu et al., 2021).

Furthermore, the selection of specific activation conditions was guided by the obtained thermogravimetric analysis results. These results indicated that activation times exceeding 87 minutes

Table 1. Physical characteristics of macadamia nut shell activated carbon at various activation temperatures and time

Temperature (°C)	Activation times (min)	Yield (%)	S_{BET} (m^2/g)	V_{total} (cm^3/g)	Mean pore diameter (nm)
900	60	70.78 ± 3.81	418.39	0.2638	2.4456
900	120	66.14 ± 3.45	502.89	0.3104	2.2537
950	60	67.32 ± 2.63	454.54	0.2678	2.3566
950	120	50.31 ± 2.93	524.69	0.3296	2.5092
950	180	44.17 ± 2.31	528.06	0.4718	2.5758
1000	60	73.37 ± 3.14	226.52	0.1131	1.9972
1000	240	56.83 ± 4.05	295.1	0.2017	2.7343

Table 2. The parameters of BET analysis of the AC-M at 950 °C of activation temperature

Samples	Activation conditions		Yield	S_{BET}	V_{Total} (cm^3/g)	D_p
	CO_2 flow (ml/min)	Time (min)	(%)	(m^2/g)		(nm)
AC-$M_{100.60}$	100	60	67.32 ± 2.21	454.54	0.27	2.36
AC-$M_{100.120}$	100	120	50.31 ± 4.52	524.69	0.33	2.51
AC-$M_{100.180}$	100	180	44.17 ± 4.64	528.06	0.34	2.58
AC-$M_{100.240}$	100	240	34.53 ± 4.03	917.71	0.47	2.06
AC-$M_{200.60}$	200	60	66.86 ± 2.79	448.92	0.28	2.40
AC-$M_{200.120}$	200	120	46.63 ± 3.29	609.98	0.36	2.43
AC-$M_{200.180}$	200	180	40.87 ± 6.86	921.69	0.45	2.23
AC-$M_{200.240}$	200	240	31.33 ± 3.94	1,363.75	0.69	2.36

and temperatures above 900 °C were highly effective in promoting the decomposition of hemicellulose, cellulose, and lignin. Such conditions, which resulted in a mass loss greater than 60% during the TGA, were deemed essential for producing adsorbents with highly favourable characteristics. Notably, the samples designated as AC-$M_{100,240}$, AC-$M_{200,180}$, and AC-$M_{200,240}$ exhibited impressive BET surface areas ranging from 917.71 to 1,363.75 m^2/g and total pore volumes from 0.45 to 0.69 cm^3/g. This definitively confirms that heightened carbon loss, driven by more rigorous activation, significantly contributes to the creation and enlargement of pores. Such high values for these porous parameters are directly linked to an increased potential for enhanced adsorption rates (Son and Park, 2020). Regarding the mean pore diameter, all AC-M samples displayed values ranging from 2.06 to 2.36 nm. Following the standards defined by the International Union of Pure and Applied Chemistry (IUPAC), pores with sizes between 2 and 50 nm are categorized as mesopores, while those smaller than 2 nm are considered micropores (Leng et al., 2021). The average values obtained for the obtained AC-M samples suggest that the produced activated carbon possesses predominantly micro-mesoporous characteristics. This is a highly desirable feature for the efficient adsorption of small organic molecules such as phenol. Micropores play a critical role by contributing significantly to the specific surface area available for adsorption, while mesopores are vital for accelerating the diffusion of adsorbate molecules into the deeper, internal pore structure.

Batch adsorption performance of AC-M for phenol

Determining optimal conditions for phenol adsorption

A series of batch experiments were conducted to optimize phenol adsorption by AC-M, aiming to identify the most favourable operating conditions. The study examined the effects of initial phenol concentration, contact time, pH level, and temperature on the adsorption performance of the AC-M samples.

As shown in Figures 3A and 3B, adsorption capacity notably increased with higher initial phenol concentrations and longer contact times. The rapid uptake observed at the beginning is largely due to a strong concentration gradient,

which facilitates mass transfer from the solution to the plentiful active sites available on the AC-M surface (Yimrattanabovorn., 2024; Saigl et al., 2023; Zhang et al., 2021). Elevated concentration enhances the driving force for mass transfer, and when combined with the abundance of active sites, this enhances the swift movement of phenol molecules into the adsorbent pores (Allahkarami et al., 2023). However, the rate of adsorption enhancement progressively slowed down at higher concentrations. This deceleration signals that the adsorption system was approaching equilibrium, as the available active sites on the AC-M surface gradually became saturated with phenol molecules (Wang et al., 2020; Dehmani et al., 2022). Upon reaching this saturation point, the diminished availability of binding sites results in a reduced overall adsorption capacity per unit mass of the adsorbent. Ultimately, an impressive maximum adsorption capacity of approximately 213 mg/g was achieved with the AC-$M_{200,240}$ sample when the initial phenol concentration was 200 mg/L and the contact time was 600 minutes. These specific conditions were identified as optimal, striking an ideal balance between effective phenol removal and efficient adsorbent utilisation, and were subsequently adopted for all further experimental work.

Phenol adsorption is strongly affected by the pH of the solution, which influences both the surface charge of the adsorbent and the chemical form of the adsorbate. Figure 3C clearly depicts the impact of varying initial pH values on AC-M adsorption capability. A notable increase in adsorption capacity was recorded as the pH escalated from 2 to 6, reaching a peak of 234.88 mg/g for AC-$M_{200,240}$ at pH 6 (compared to 143.28 mg/g at pH 2). This behaviour can be rationalised by considering the AC-M's point of zero charge (pH_{pzc}), which was determined to be 8.70. At pH levels below 8.7, the AC-M surface primarily carries a positive charge due to protonation. Consequently, at the chosen optimal pH of 6, phenol molecules largely exist in their undissociated (molecular) form C_6H_5OH, rather than as negatively charged phenoxide ions ($C_6H_5O^-$). This slight positive charge on the AC-M surface at pH 6 does not repel the non-ionic phenol, thereby favouring strong hydrophobic interactions and hydrogen interaction between the uncharged phenol and the hydrophobic carbon surface of AC-M. In contrast, a considerable decline in adsorption capacity was noted at pH levels below 6. Under highly acidic conditions, despite phenol remaining molecular, competitive adsorption by an excess of H^+ ions on the AC-M surface might impede phenol uptake. Furthermore, if sulfuric acid is employed for pH adjustment, the potential formation of phenol disulphonic acid could

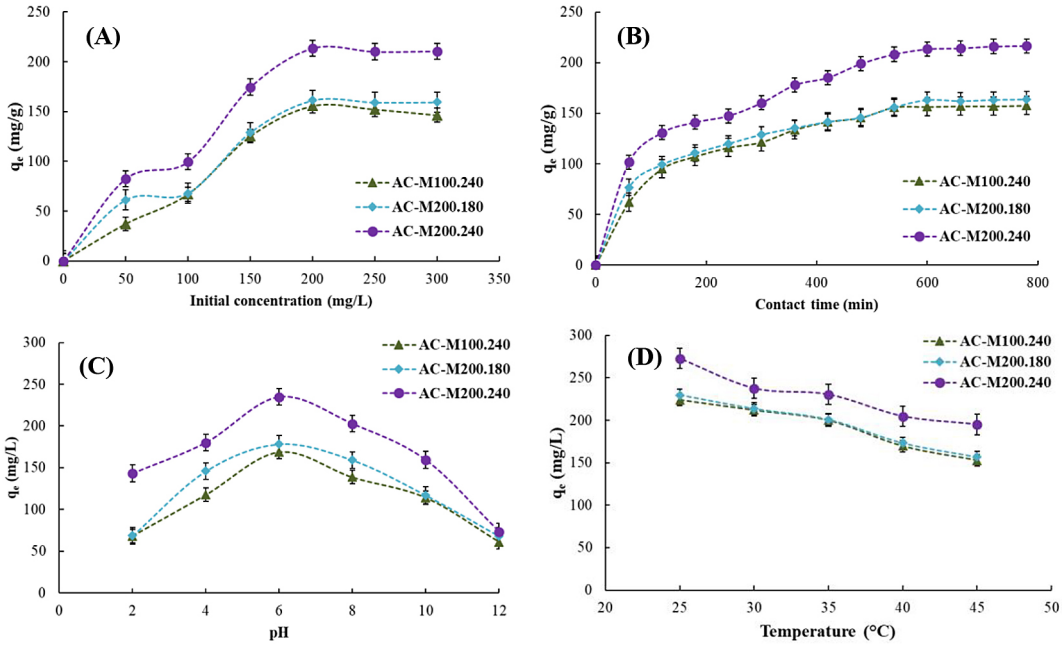

Figure 3. Effects of (A) initial phenol concentration, (B) contact time, (C) solution pH, (D) temperature on phenol adsorption capacity (q_e) of AC-M

alter adsorption characteristics. Conversely, elevating the pH to 12 resulted in a sharp decline in adsorption capacity, plummeting to 73.55 mg/g. At such highly alkaline pH (i.e., pH > pKa of phenol), phenol predominantly deprotonates into negatively charged phenoxide ions ($C_6H_5O^-$) (Xie et al., 2020). At pH levels above the point of zero charge (pH_{pzc} = 8.7), the AC-M surface becomes negatively charged, resulting in strong electrostatic repulsion with anionic phenoxide ions, which significantly hinders the adsorption process. Therefore, pH 6 was chosen as the optimal condition for all following adsorption studies.

The effect of temperature on the capacity of AC-M to absorb phenol was investigated within a range of 25 to 45 °C, with the results detailed in Figure 3D. The rise in temperature from 25 °C to 45 °C led to a steady decrease in adsorption capacity for AC-M200.240, dropping from 272.72 mg/g to 195.09 mg/g. This inverse correlation between temperature and adsorption capacity indicates that the adsorption of phenol onto AC-M is an exothermic process. In an exothermic adsorption mechanism, an increase in temperature provides adsorbate molecules with greater kinetic energy, leading to more rapid movement. This increased thermal energy weakens the attractive forces between the adsorbate (phenol) and the adsorbent (AC-M) surface, making it easier for adsorbed molecules to desorb back into the solution rather than remaining bound. Consequently, the overall adsorption capacity is diminished. Moreover, the decline in adsorption with rising temperature suggests that the process is largely physical adsorption, involving weaker intermolecular forces such as van der Waals forces or hydrogen bonds, which are typically disrupted by higher thermal energy. On the basis of these findings, a temperature of 25 °C was chosen as the optimal condition for all subsequent experiments to ensure maximum phenol removal efficiency.

However, the practical application of activated carbon from macadamia nut shell for real industrial wastewater treatment necessitates considering the impact of complex coexisting compounds, such as heavy metals, total organic carbon (TOC), or surfactants. These contaminants might affect the phenol removal efficiency through competitive adsorption mechanisms or surface fouling. Therefore, future research should focus on evaluating the performance of AC-M in wastewater matrices containing coexisting contaminants to truly confirm its industrial applicability.

Adsorption isotherm modelling for batch studies

To obtain a detailed understanding of the equilibrium properties of phenol adsorption onto AC-M, the experimental data from the conducted batch studies were rigorously analysed using the Langmuir and Freundlich adsorption isotherms. Equilibrium modelling was performed under carefully controlled conditions based on prior optimisation results: 200 mg/L initial phenol concentration, 600 minutes of contact time, pH 6, agitation at 200 rpm, and a constant temperature of 25 °C. To generate the full isotherm data, varying quantities of AC-M adsorbent (ranging from 0.02 to 0.5 g) were employed.

The fitting results, summarised in Table 3, unequivocally demonstrated that the Langmuir isotherm model provided a significantly superior fit to the experimental data compared to the Freundlich isotherm model. The coefficients of determination (R^2) for the Langmuir model ranged from 0.9723 to 0.9949, which were notably higher than those obtained for the Freundlich model (ranging from 0.8961 to 0.9941). This strong correlation with the Langmuir isotherm strongly suggests that phenol adsorption onto AC-M predominantly occurs as monolayer coverage on a homogeneous surface. This implies that the adsorption sites are distinct, independent, and possess uniform energy levels, with minimal significant interactions between adsorbed molecules. Furthermore, the maximum theoretical adsorption capacity (q_{max}) derived from the Langmuir model was impressively high, reaching 588.24 mg/g for the AC-M200.240 sample. This exceptional adsorption capacity of AC-$M_{200,240}$ is directly attributable to its superior porous properties, specifically its remarkable surface area (1,363.75 m^2/g) and substantial total pore volume (0.69 cm^3/g), as previously verified by BET analysis (Table 2). These well-developed porous structures furnish an abundance of highly accessible active sites for phenol molecules, thereby significantly bolstering overall adsorption performance.

When compared to other activated carbons derived from the agricultural waste reported in the literature, AC-$M_{200.240}$ demonstrates superior performance. Previous studies have reported phenol adsorption capacities of 341.00 mg/g for macadamia nut shell (Rodrigues et al., 2013), 26.95 mg/g

Table 3. The constants and adsorption capacity by Langmuir and Freundlich isotherms

Sample	Langmuir constants			Freundlich constants		
	q_{max} (mg/g)	K_L (mg/g)	R^2	K_F (mg/g)	N	R^2
AC-$M_{100.240}$	322.58	0.05299	0.9949	52.19	2.89	0.9922
AC-$M_{200.180}$	370.37	0.09215	0.9942	80.67	3.38	0.9941
AC-$M_{200.240}$	588.24	0.05923	0.9723	127.44	3.92	0.8961

for banyan root (Nirmala et al., 2019), 98.60 mg/g for black wattle bark waste (Lutke et al., 2019), and 96.92 mg/g for acacia mangium (Zhang et al., 2021). This comparison clearly demonstrates that AC-$M_{200.240}$ exhibits significantly higher adsorption capacity than these previously reported materials.

These findings indicate that AC-M200.240 has exceptional potential as a raw material for producing high-performance activated carbon for phenol removal from industrial wastewater applications.

Phenol removal via continuous flow adsorption in a fixed-bed column

Impact of operational parameters on fixed-bed column performance

Our investigation into phenol adsorption in a continuous fixed-bed column system utilised 13 ± 0.05 g of AC-$M_{200.240}$, which had previously demonstrated the highest adsorption capacity in batch experiments. The fixed-bed system was operated using conditions based on the optimal parameters identified in the batch experiments: phenol concentration of 200 mg/L, a contact duration of 60 minutes, a starting pH of 6, and a temperature maintained between 25 and 30 °C.

The fixed-bed column experiments were conducted under varying initial phenol concentrations, as summarised in Table 4. A distinct pattern was observed, raising the initial phenol concentration from 150 to 200 and then to 250 mg/L led to a significant decline in both the breakthrough time (t_b), which dropped from 26 to 18 hours, and the saturation time (t_s), which decreased from 74 to 44 hours. This hastened saturation at higher concentrations is primarily attributable to the enhanced driving force, which accelerates the mass transfer and adsorption rate of phenol molecules onto the AC-M surface, leading to a quicker occupation of available pores and active sites (Daffalla et al., 2022).

Figure 4 illustrates this relationship by plotting the normalised effluent concentration (C/C_0) against time. It demonstrates that a decrease in the initial phenol concentration causes the breakthrough curves to shift significantly from left to right, becoming notably gentler in slope. This visual representation directly correlates with extended breakthrough and saturation times (Vidovix et al., 2022). Similarly, Figure 5 depicts the impact of increasing flow rates (4, 5, and 6 mL/min). Higher flow rates led to a reduction in both breakthrough time and the overall adsorption capacity (q_e), as detailed in Table 3, where q_e noticeably dropped from 270.25 to 239.81 mg/g. This decline is attributed to the reduced contact time between phenol molecules and the AC-M surface at higher flow velocities, which restricts the effective diffusion of phenol into the pores and limits interaction with active adsorption sites (Nedjai et al., 2024).

In contrast, utilising a lower flow rate for example, 4 mL/min prolongs the contact time between the adsorbate and adsorbent. This extended interaction promotes deeper diffusion and more efficient adsorption, ultimately increasing the adsorption capacity and prolonging the operational duration of the column (Yimrattanabovorn et al., 2024; Feizi et al., 2021). The resulting smoother and more gradual breakthrough curves further underscore improved adsorption performance due to the extended residence time of phenol molecules on the AC-M surface. Under the optimal conditions of a 4 mL/min flow rate and phenol concentration of 250 mg/L, the system achieved a maximum adsorption capacity of 270.25 mg/g under equilibrium conditions. The breakthrough graph for this setup initially exhibited a steep increase, which gradually levelled off as the AC-M bed neared saturation, reflecting a slower adsorption rate in the later stages.

Kinetic modelling of fixed-bed adsorption

To thoroughly assess the kinetic and adsorption characteristics of phenol within the fixed-bed column system and to forecast the adsorption capacity of the column, the experimental breakthrough curve data were rigorously analysed using the Thomas and Yoon-Nelson models. The

Table 4. The parameters and adsorption capacity of fixed-bed column

C_0 (mg/L)	Q (ml/min)	L_{MTZ} (cm)	t_b (hr)	t_e (hr)	q_b (mg/g)	q_e (mg/g)
150	6	6.5	26.0	74.0	93.09	201.57
200	6	7.0	20.0	66.0	98.68	225.03
250	6	5.9	18.0	44.0	123.91	239.81
250	5	5.5	25.0	56.0	133.53	255.28
250	4	5.2	31.0	64.0	145.70	270.25

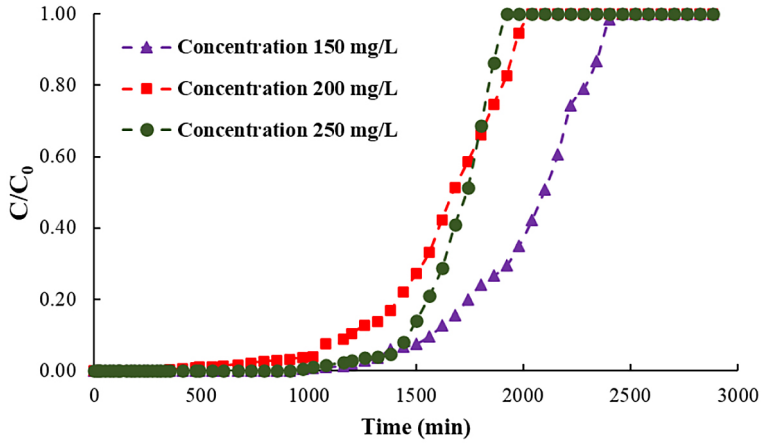

Figure 4. Phenol adsorption breakthrough curves for fixed-bed column under varying initial phenol concentrations

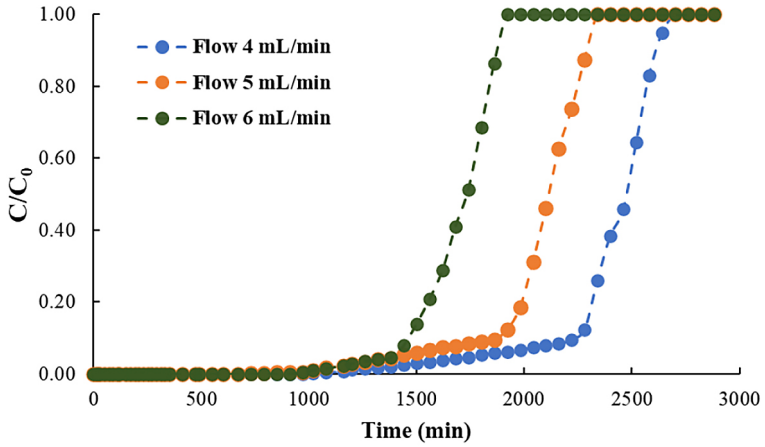

Figure 5. Phenol adsorption breakthrough curves for fixed-bed column under varying flow rate

derived parameters from both models, along with their respective coefficients of determination (R^2), are meticulously presented in Table 5.

The conducted analysis revealed that the Thomas model consistently produced the R^2 values ranging from 0.9669 to 0.9908. These values were notably higher than those obtained from the Yoon-Nelson model, which yielded R^2 values between 0.9555 and 0.9883. This superior statistical fit strongly suggests that the Thomas model provides a more accurate representation of the experimental data and is thus more effective in describing the adsorption behaviour observed within our fixed-bed column system. This finding aligns well with previous research, which has frequently shown the Thomas model to be highly suitable for predicting breakthrough curves in fixed-bed adsorption processes, especially when the process is governed by interfacial mass transfer. Furthermore, it is hypothesised

Table 5. The adsorption capacity of fixed-bed column studies investigated with the Thomas and Yoon-Nelson model

C_0 (mg/L)	Flowrate (ml/min)	Bed heights (cm)	Thomas model			Yoon-Nelson model		
			k_{TH} (L/mg-min)	q_{TH} (mg/g)	R^2	k_{YN} (min^{-1})	τ (hr)	R^2
150	6	10	0.0260	146.29	0.9906	0.0048	33.85	0.9883
200	6	10	0.0140	198.53	0.9908	0.0043	28.02	0.9825
250	6	10	0.0247	233.58	0.9725	0.0057	25.59	0.9555
250	5	10	0.0086	241.71	0.9669	0.0022	40.75	0.9669
250	4	10	0.0066	251.47	0.9882	0.0020	49.15	0.9723

that the adsorption process is non-reversible and conforms to Langmuir isotherm equilibrium. This assumption is notably supported by the isotherm results obtained from the batch adsorption experiments conducted in this study. Regarding the impact of operational variables, the Thomas model-predicted adsorption capacity (q_{TH}) showed a direct correlation with the initial phenol concentration. As the initial phenol concentration increased, the q_{TH} value rose from 146.29 to 233.58 mg/g. Conversely, an increase in the flow rate resulted in a decrease in q_{TH}, with values dropping from 251.47 to 233.58 mg/g. This behaviour is consistent with our experimental observations, which indicated that lower flow rates prolong the contact time between phenol and the adsorbent, thereby leading to more efficient adsorption and ultimately higher adsorption capacities.

Enhanced phenol adsorption and extended lifespan using a partial-bed column system

Continuous flow adsorption of phenol on partial-bed column

The efficacy of the partial-bed column system for phenol adsorption was investigated under conditions optimised from the conducted fixed-bed studies, specifically utilizing an initial phenol concentration of 250 mg/L and a flow rate of 4 mL/min. Different partial-bed removal heights (2, 4, and 6 cm) were systematically examined to evaluate their influence on adsorption capacity and the operational longevity of the column. In this dynamic system, once the effluent concentration reached 50% of the influent (C_e/C_0 = 0.50), the corresponding saturated bed height was extracted and replenished with fresh AC-M from the top of the column.

This study encompassed three distinct adsorption cycles, with the key breakthrough curve parameters meticulously summarised in Table 6. The results reveal a distinct relationship between the height of the removed adsorbent layer (2, 4, and 6 cm) and improved adsorption performance. The adsorption efficiency ($q_{0.5}$) increased accordingly, reaching 217.04, 236.60, and 246.70 mg/g, respectively. As depicted in Figures 6a–c, higher removed bed heights caused the breakthrough curves to progressively shift to the right, yielding corresponding $t_{0.5}$ values of 72.67, 98.33, and 124.00 hours. The increasingly gentle slopes of these breakthrough curves are indicative of prolonged breakthrough and saturation times (Li et al., 2023). Consequently, the operational lifespan of the partial-bed column was dramatically extended from 39.00 hours (observed in the conventional fixed-bed column) to an impressive 124.00 hours.

A detailed examination revealed that the duration of the first cycle in the partial-bed experiment, across all adsorbent removal heights (2, 4, and 6 cm), was approximately 39.00 hours a value closely mirroring that obtained from the fixed-bed column, primarily because both initiated with an identical effective bed height of 10 cm. However, a remarkable increase in cycle duration was observed in the subsequent cycles: in the second cycle, durations extended to 52.50, 64.50, and 76.50 hours for removal heights of 2, 4, and 6 cm, respectively. The third cycle further prolonged these durations to 72.67, 98.33, and 124.00 hours, unequivocally showing that cycles 2 and 3 facilitated substantially longer operational periods compared to cycle 1. This consistent positive trend is further substantiated by the data presented in Table 6, which encapsulates the breakthrough curve parameters for the partial-bed system. The data unequivocally highlight a continuous increase in both breakthrough (q_b) and half-saturation ($q_{0.5}$) adsorption capacities with each successive cycle and with greater adsorbent removal heights. The enhanced operational time and adsorption capacity observed in cycles 2 and 3 of the partial-bed

system, relative to both cycle 1 and the fixed-bed column, can be primarily ascribed to the system's inherent ability to conserve the unsaturated upper layer of the adsorbent. This unique feature allows for the selective removal and replacement of only the saturated bottom portion with fresh material. This contrasts sharply with the fixed-bed system, where the entire adsorbent bed must be replaced once saturation is achieved.

Moreover, systematically increasing the height of the removed adsorbent in each cycle significantly augments the contact time between phenol and the adsorbent. This extended interaction period provides phenol molecules with more ample opportunity to diffuse effectively into the internal pore structure and bind securely to available adsorption sites, resulting in a higher overall adsorption capacity and a prolonged column lifespan. These findings are consistent with the observations of (Yimrattanabovorn et al., 2024), whose work reported a progressive decrease in total porosity by volume of AC-M in a partial-bed system across cycles (from fresh to spent AC-M), indicating effective utilisation of the adsorbent. Their research also confirmed that the top layer of the bed during each cycle maintained enough active sites to ensure continued efficient adsorption.

Considering the concept of the Mass Transfer Zone (L_{MTZ}) in a fixed-bed adsorption column, as the adsorbate flows through, the adsorbent gradually saturates from the inlet towards the outlet, forming an L_{MTZ} where the majority of adsorption occurs. Over time, this L_{MTZ} migrates along the column length until phenol begins to break through, eventually leading to complete column saturation. In the partial-bed system, when the lower, saturated segment of the L_{MTZ} is removed, and fresh adsorbent is introduced, the unsaturated L_{MTZ} can be continuously maintained within the column (Yimrattanabovorn et al., 2024). This ingenious mechanism ensures optimal utilisation of the adsorbent, as the newly added material continues to perform at its peak capacity, thereby greatly extending the operational life of the column. Although adsorbent is periodically removed, the continuous introduction of fresh adsorbent effectively maintains or even increases the active bed height, which boosts the number of available active sites and extends the exposure duration between the adsorbate and adsorbent (Plangklang and Sookkumnerd, 2023). This provides phenol molecules sufficient time for efficient diffusion through the liquid film surrounding the particles (film diffusion) and into the adsorbent pores (intraparticle diffusion) to achieve complete binding with internal adsorption sites. Furthermore, regarding the mitigation of saturation effects, while a fixed-bed system experiences a rapid decline in overall adsorption efficiency once a portion of its adsorbent becomes saturated, the partial-bed system can periodically "rejuvenate" its adsorption capacity by removing saturated material and integrating fresh adsorbent. This allows the column to sustain its treatment efficiency for longer durations and ultimately achieve a higher overall adsorption capacity in the long run (Patel, 2022). Comparatively, the partial-bed system, with adsorbent removal heights of 2, 4, and 6 cm, exhibited significantly higher adsorption capacities than the fixed-bed system, showcasing increases of 27.39%, 38.87%, and 44.79%, respectively. Notably, at a 6 cm removal height, the partial-bed column achieved an extended operational time

Table 6. Evaluation of breakthrough parameters for phenol removal on AC-M in a partial-bed column

Partial-bed height (cm)	Cycle	L_{MTZ} (cm)	t_b (hr)	$t_{0.5}$ (hr)	q_b (mg/g)	$q_{0.5}$ (mg/g)
0	1	5.16	31.00	39.00	139.51	170.38
2	1	2.05	31.00	39.00	142.39	168.27
	2	4.11	43.50	52.50	157.32	185.42
	3	6.74	59.00	72.67	180.08	217.04
4	1	2.05	31.00	39.00	144.30	170.71
	2	4.73	52.17	64.50	165.74	200.00
	3	8.33	78.67	98.33	192.34	236.60
6	1	2.05	31.00	39.00	141.52	168.66
	2	4.91	62.83	76.50	174.37	209.30
	3	8.99	101.00	124.00	203.83	246.70

of 124 hours, a remarkable improvement compared to just 39 hours for the 10 cm fixed-bed column. These compelling results emphatically underscore the superior efficiency of the partial-bed system in prolonging adsorbent lifespan and enhancing overall adsorption performance, which ultimately contributes to lower operational costs and improved sustainability of the wastewater treatment process. While the partial-bed adsorption system concept offers advantages for continuous operation and system modularity, its industrial application still faces significant operational limitations that warrant consideration. These include the inherent complexity of designing robust and fully automated systems for continuous adsorbent exchange without disrupting the flow. Furthermore, the physical properties of the adsorbent particles, such as their density and size relative to the feed flow rate, are critical for maintaining a stable bed and preventing excessive fluidisation or channelling. There is also a potential risk of clogging or fouling over long

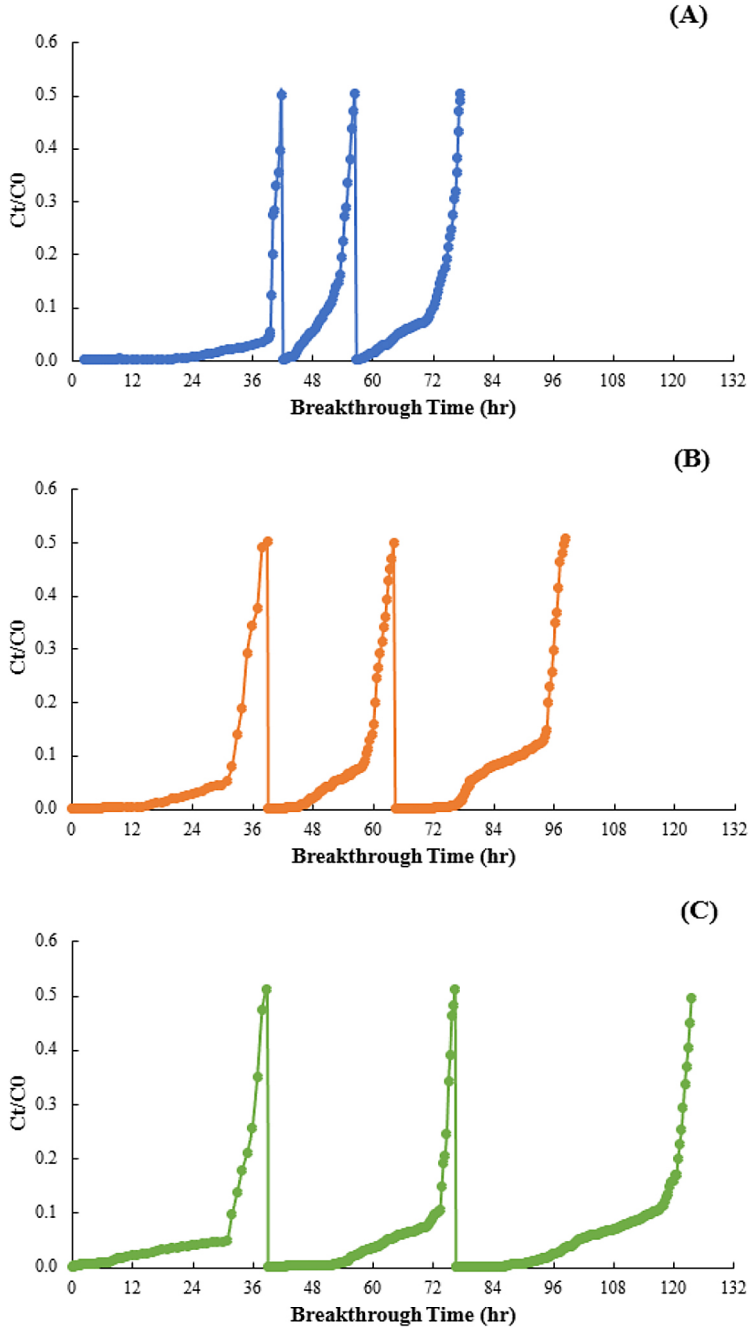

Figure 6. Breakthrough curves of phenol adsorption in a partial-bed column at different removed-bed heights (A) 2 cm., (B) 4 cm., (C) 6 cm

operational periods, depending on the wastewater characteristics. Consequently, scaling up the system from laboratory to industrial scale presents complex engineering challenges that necessitate further pilot-scale investigation and optimisation of the engineering design.

Kinetic modelling of partial-bed adsorption: Thomas and Yoon-Nelson column models

To gain deeper insight into the adsorption kinetics and forecast the behaviour of phenol removal in the partial-bed column, the breakthrough data were analysed using the Thomas and Yoon–Nelson models. The calculated parameters from these models, along with their corresponding determination coefficients (R^2), are presented in Table 7.

Our analysis exhibited that the Thomas model consistently provided a superior fit to the experimental data. Its R^2 values ranged from 0.8753 to 0.9598, significantly higher than those from the Yoon-Nelson model, which ranged from 0.2822 to 0.3313. This disparity indicates that the Thomas column model is more effective at describing the observed phenol adsorption behaviour in the studied partial-bed column.

Specifically, for the Thomas model, the theoretical maximum adsorption capacity (q_{TH}) exhibited a positive correlation with increased operational cycles and larger adsorbent removal heights (2, 4, 6 cm). For example, at a 6 cm removal height, q_{TH} increased from 224.77 mg/g in Cycle 1 to 322.90 mg/g in Cycle 2, and further to 386.76 mg/g in Cycle 3. This trend strongly aligns with the experimental findings, which demonstrated improved column efficiency in later cycles. This improvement is a direct result of the system's ability to remove saturated adsorbent and replenish it with fresh material, thereby preserving the unsaturated Mass Transfer Zone (L_{MTZ}) and extending the overall operational lifespan of the column.

CONCLUSIONS

This comprehensive investigation decisively demonstrates the superior efficacy and sustainability of activated carbon (AC-M) derived from macadamia nut shells, unequivocally establishing its significant potential as a cost-effective adsorbent. This research highlights a valuable pathway for the utilisation of agricultural waste in environmental remediation. The AC-M, synthesised under optimised conditions, specifically at 950 °C with a controlled CO_2 flow of 200 mL/min for 240 minutes proved to be an exceptional adsorbent. It exhibited ideal textural properties, characterised by an impressive BET surface area of up to 1,363.75 m^2/g.

Batch adsorption experiments accurately determined the ideal conditions for efficient phenol removal. The experimental results closely fit the Langmuir isotherm model, confirming a favourable monolayer adsorption process and indicating a high theoretical maximum adsorption capacity of 588.24 mg/g for the most effective AC-M sample.

The partial-bed column system demonstrated a remarkable improvement compared to traditional fixed-bed setups. Notably, operating with a 6 cm removal height of the adsorbent layer extended the column service time to 124 hours and increased the adsorption capacity to 246.70 mg/g. This represents a remarkable 39.89% increase in adsorption capacity compared to the fixed-bed

Table 7. Assessment of phenol adsorption in a partial-bed column via Thomas and Yoon-Nelson Models

Partial-bed height (cm)	Cycle	Bed height (cm)	Thomas model			Yoon-Nelson model		
			k_{TH} (L/mg-min)	q_{TH} (mg/g)	R^2	k_{YN} (min^{-1})	τ (hr)	R^2
2	1	10	0.0161	168.08	0.9399	0.0038	38.72	0.9399
	2	12	0.0267	316.96	0.9095	0.0063	52.84	0.9095
	3	14	0.0166	235.93	0.8753	0.0039	74.13	0.8753
4	1	10	0.0133	192.87	0.973	0.0034	40.80	0.973
	2	14	0.0183	303.33	0.9554	0.0047	64.99	0.9554
	3	18	0.0140	270.31	0.912	0.0036	97.22	0.912
6	1	10	0.0079	224.77	0.9157	0.0020	47.93	0.9157
	2	16	0.0106	322.90	0.9598	0.0027	81.61	0.9598
	3	22	0.0114	386.76	0.8949	0.0029	125.14	0.8949

system, unequivocally highlighting a more efficient utilisation of the adsorbent potential over prolonged periods. This research strongly advocates for the adoption of partial-bed column technology as a next-generation approach for continuous adsorption processes, effectively leveraging the untapped potential of renewable adsorbents for long-term environmental protection. To fully realise the sustainable industrial applicability of this approach, future studies should also focus on evaluating and developing effective regeneration methods for the spent macadamia nut shell AC-M, which is a critical factor for both economic feasibility and minimising the overall environmental impact of the phenol adsorption process.

Acknowledgements

This research was financially supported by (i) Suranaree University of Technology (SUT), (ii) Thailand Science Research and Innovation (TSRI), and (iii) National Science, Research and Innovation Fund (NSRF) (Project ID: NRIIS 204176).

REFERENCES

1. Allahkarami E., Dehghan Monfared A., Silva L.F.O., Dotto G.L. (2023). Toward a mechanistic understanding of adsorption behavior of phenol onto a novel activated carbon composite. *Scientific Reports*, *13*(1), 167. https://doi.org/10.1038/s41598-023-27507-5
2. Annually, R.I. (1995). *Astm standards*.
3. Daffalla S.B., Mukhtar H., Shaharun M.S., Hassaballa A.A. (2022). Fixed-bed adsorption of phenol onto microporous activated carbon set from rice husk using chemical activation. *Applied Sciences*, *12*(9), 4354. https://doi.org/10.3390/app12094354
4. Dehmani Y., Dridi D., Lamhasni T., Abouarnadasse S., Chtourou R., Lima E.C. (2022). Review of phenol adsorption on transition metal oxides and other adsorbents. *Journal of water process engineering*, *49*, 102965. https://doi.org/10.1016/j.jwpe.2022.102965
5. Dittmann D., Saal L., Zietzschmann F., Mai M., Altmann K., Al-Sabbagh D., Braun U. (2022). Characterization of activated carbons for water treatment using TGA-FTIR for analysis of oxygen-containing functional groups. *Applied Water Science*, *12*(8), 203. https://doi.org/10.1007/s13201-022-01723-2
6. Eryılmaz C., Genç A. (2021). Review of treatment technologies for the removal of phenol from wastewaters. *Journal of Water Chemistry and Technology, 43*(2), 145–154. https://doi.org/10.3103/S1063455X21020065
7. Feizi F., Sarmah A.K., Rangsivek R. (2021). Adsorption of pharmaceuticals in a fixed-bed column using tyre-based activated carbon: Experimental investigations and numerical modelling. *Journal of Hazardous Materials*, *417*, 126010. https://doi.org/10.1016/j.jhazmat.2021.126010
8. Heidarinejad Z., Dehghani M.H., Heidari M., Javedan G., Ali I., Sillanpää M. (2020). Methods for preparation and activation of activated carbon: a review. *Environmental Chemistry Letters*, *18*, 393–415. https://doi.org/10.1007/s10311-019-00955-0
9. Leng L., Xiong Q., Yang L., Li H., Zhou Y., Zhang W., Huang H. (2021). An overview on engineering the surface area and porosity of biochar. *Science of the total Environment*, *763*, 144204. https://doi.org/10.1016/j.scitotenv.2020.144204
10. Li Y., Gong F., Yang W., Liu B. (2023). Effective triclosan removal by using porous aromatic frameworks in continuous fixed-bed column studies. *Environmental Science and Pollution Research, 30*, 121007–121013. https://doi.org/10.1007/s11356-023-30714-2
11. Lütke, S.F., Igansi, A.V., Pegoraro, L., Dotto, G.L., Pinto, L.A., and Cadaval Jr, T.R. (2019). Preparation of activated carbon from black wattle bark waste and its application for phenol adsorption. *Journal of Environmental Chemical Engineering. 7*(5), 103396. https://doi.org/10.1016/j.jece.2019.103396
12. Mesfer M.K., Danish M., Khan M.I., Ali I.H., Hasan M., Jery A.E. (2020). Continuous fixed bed CO_2 adsorption: Breakthrough, Column Efficiency, Mass Transfer Zone. *Processes 8*(10). https://doi.org/10.3390/pr8101233
13. Mohd A. (2022). Presence of phenol in wastewater effluent and its removal: an overview. *International Journal of Environmental Analytical Chemistry, 102*(6), 1362–1384. https://doi.org/10.1080/03067319.2020.1738412
14. Nedjai R., Kabbashi N., Alam M.Z., Alkhatib M., Tahreen A., Al Mamun A. (2024). Adsorption performance of fixed-bed columns for the removal of phenol using baobab fruit shell based activated carbon. *IIUM Engineering Journal*, *25*(1), 59–71. https://doi.org/10.31436/iiumej.v25i1.2932
15. Nirmala, G., Murugesan, T., Rambabu, K., Sathiyanarayanan, K., and Show, P.L. (2021). Adsorptive removal of phenol using banyan root activated carbon. *Chemical Engineering Communications. 208*(6), 831–842. https://doi.org/10.1080/00986445.2019.1674839
16. Patel H. (2019). Fixed-bed column adsorption study: a comprehensive review. Appl Water Sci, 9(45). https://doi.org/10.1007/s13201-019-0927-7
17. Patel, H. (2022). Comparison of batch and fixed bed column adsorption: a critical review. *International*

Journal of Environmental Science and Technology, *19*(10), 10409–10426. https://doi.org/10.1007/s13762-021-03492-y

18. Plangklang C., Sookkumnerd T. (2023). Modelling and feedforward control of pulsed bed adsorption column for colorant removal in sugar syrup. *Engineering Journal*, *27*(1), 29–38. https://doi.org/10.4186/ej.2023.27.1.29
19. Rasapoor M., Young B., Asadov A., Brar R., Sarmah A.K., Zhuang W.Q., Baroutian S.J.E. C. (2020). Effects of biochar and activated carbon on biogas generation: A thermogravimetric and chemical analysis approach. *Energy Conversion and Management, 203*, 112221. https://doi.org/10.1016/j.enconman.2019.112221
20. Rodrigues, L.A., de Sousa Ribeiro, L.A., Thim, G.P., Ferreira, R.R., Alvarez-Mendez, M.O., and dos Reis Coutinho, A. (2013). Activated carbon derived from macadamia nut shells: an effective adsorbent for phenol removal. *Journal of Porous Materials. 20*(4), 619–627. https://doi.org/10.1007/s10934-012-9635-5
21. Said K.A.M., Ismail A.F., Karim Z.A., Abdullah M.S., Hafee, A. (2021). A review of technologies for the phenolic compounds recovery and phenol removal from wastewater. *Process Safety and Environmental Protection, 151*, 257–289. https://doi.org/10.1016/j.psep.2021.05.015
22. Saigl Z., Tifouti O., Alkhanbashi B., Alharbi G., Algamdi H. (2023). Chitosan as adsorbent for removal of some organic dyes: A review. *Chemical Papers*, *77*(5), 2363–2405. https://doi.org/10.1007/s11696-022-02641-y
23. Saputera W.H., Putrie A.S., Esmailpour A.A., Sasongko D., Suendo V., Mukti R.R. (2021). Technology advances in phenol removals: Current progress and future perspectives. *Catalysts, 11*(8), 998. https://doi.org/10.3390/catal11080998
24. Sazali N., Harun Z., Sazali N. (2020). A review on batch and column adsorption of various adsorbent towards the removal of heavy metal. *Journal of Advanced Research in Fluid Mechanics and Thermal Sciences, 67*(2), 66–88.
25. Son Y.R., Park S.J. (2020). Preparation and characterization of mesoporous activated carbons from nonporous hard carbon via enhanced steam activation strategy. *Materials Chemistry and Physics*, *242*, 122454. https://doi.org/10.1016/j.matchemphys.2019.122454
26. Vidovix T.B., Januário E.F.D., Araújo M.F., Bergamasco R., Vieira A.M.S. (2022). Investigation of two new low-cost adsorbents functionalized with magnetic nanoparticles for the efficient removal of triclosan and a synthetic mixture. *Environmental Science and Pollution Research, 29*, 46813–46829. https://doi.org/10.1007/s11356-022-19187-x
27. Wang L., Shi C., Pan L., Zhang X., Zou J. J. (2020). Rational design, synthesis, adsorption principles and applications of metal oxide adsorbents: a review. *Nanoscale*, *12*(8), 4790–4815. https://doi.org/10.1039/C9NR09274A
28. Wongcharee S., Aravinthan V., Erdei L., Sanongraj W. (2018). Mesoporous activated carbon prepared from macadamia nut shell waste by carbon dioxide activation: Comparative characterisation and study of methylene blue removal from aqueous solution. Asia-Pac J Chem Eng, 13. https://doi.org/10.1002/apj.2179
29. Xie, B., Qin, J., Wang, S., Li, X., Sun, H., and Chen, W. (2020). Adsorption of phenol on commercial activated carbons: modelling and interpretation. *International journal of environmental research and public health. 17*(3), 789. https://doi.org/10.3390/ijerph17030789
30. Xu H., Sun X., Yang H., Cui J., Wang J., Kang Y., Huang G. (2024). Degradation of aqueous phenol by combined ultraviolet and electrochemical oxidation treatment. *Journal of Cleaner Production, 436*, 140672. https://doi.org/10.1016/j.jclepro.2024.140672
31. Yimrattanabovorn J., Phalaiphai M. and Nawong S. (2024). Pulsed-bed column adsorption for triclosan removal using macadamia nut shell activated carbon. *Civil Engineering Journal Iran, 10*(5), 1645–1661. https://doi.org/10.28991/CEJ-2024-010-05-019
32. Zhang J., Qin L., Yang Y., Liu X. (2021). Porous carbon nanospheres aerogel based molecularly imprinted polymer for efficient phenol adsorption and removal from wastewater. *Separation and Purification Technology*, *274*, 119029. https://doi.org/10.1016/j.seppur.2021.119029
33. Zhang, F., Zhang, S., Chen, L., Liu, Z., and Qin, J. (2021). Utilization of bark waste of *Acacia mangium*: The preparation of activated carbon and adsorption of phenolic wastewater. *Industrial Crops and Products. 160*, 113157. https://doi.org/10.1016/j.